Deterministic lattice Lorentz gas. I. Chiral model

1991 J. Phys. A: Math. Gen. 24 787

(http://iopscience.iop.org/0305-4470/24/4/014)

J. Phys. A: Math. Gen. 24 (1991) 787–806. Printed in the UK

Deterministic lattice Lorentz gas: I. Chiral model

G A van Velzen

Institute for Theoretical Physics, Princetonplein 5, PO Box 80006, 3508 TA Utrecht, The Netherlands

Received 31 July 1990

Abstract. We study diffusion by using a specific type of cellular automaton, where particles move in a random environment of scatterers. The deterministic collision rules, used in the model, give rise to certain difficulties related to non-ergodicity. The class of models, introduced by Gunn and Ortuño, also contains the model studied by Gates. Previously developed theory, including the Boltzmann approximation, the ring and repeated-ring approximations and the effective medium approximation (EMA), is generalized for this model. The validity is further investigated using computer simulations. In the presence of reflecting scatterers EMA yields low-density results that show the *breakdown* of the Boltzmann equation, while they agree quantitatively with the low-density simulations. EMA also agrees with a phase transition that occurs for some parameter choices.

1. Introduction

In the context of the recent developments in discrete kinetic theory, lattice gases, cellular automata, etc [1–6] interesting features were found for the lattice Lorentz gas [7–9]. The classical Lorentz gases, consisting of ballistically moving particles that collide with randomly placed scatterers, have been used extensively in the study of diffusion phenomena [10–15]. A variety of scatterer shapes have been considered to represent the scatterering rules, such as circles or spheres, diamonds, etc. The lattice version is defined as a random quenched array of scatterers that reside on the sites of a lattice. Ballistically moving particles move mutually independently along the lines of this lattice, and scatter off the scatterers. The unit of time is chosen such that at integer values of the time the particle is at a site. For the lattice model it was demonstrated that the discrete phase space for the velocities introduces strong quasi-one-dimensional features [16–18]. The molecular chaos assumption then no longer guarantees to account for all dominant contributions to diffusion, and the Boltzmann equation *breaks down*.

The continuous Lorentz gas is a *deterministic* model: once the scatterer configuration and initial position and velocity of the moving particle are known, its whole trajectory is determined. In the present paper we study some aspects of a *lattice model* with deterministic scattering rules. This is opposed to the *stochastic* lattice Lorentz gas, where the collision rules are such that, upon hitting an impurity, the moving particle is transmitted, reflected or deflected with a certain probability. However, as the ultimate goal of kinetic theory is to derive (in the thermodynamic limit) irreversible behaviour from reversible microscopic equations of motion, one wishes to get rid of

0305-4470/91/040787+20$03.50

stochastic collision rules. In order to investigate the consequences, we discuss some deterministic lattice Lorentz gases, where the outcome of a collision depends on a *fixed* property of the scatterer. These collision properties are still to be chosen.

The chiral model, which we will discuss in this paper, was introduced by Gunn and Ortuño [19]. It is typically formulated in two dimensions; that is, it is not obvious how to generalize it for higher dimensionality.

Some general remarks can be made concerning two-dimensional deterministic models and the fundamental problems occurring here. Note that by taking the Lorentz gas we obviate the usual difficulties inherent in two-dimensional hydrodynamics. We first note that, in the ensemble of scatterer configurations, the possible trajectories of the moving particle, for given initial position and velocity, are the same for stochastic and deterministic models as long as the trajectories do not return to points visited before. However, from general random walk theory in two dimensions one concludes that there is unit probability for a random walker to return to its origin, indicating that returns should be accounted for. The return from a specified direction will thus also happen with unit probability, as the coordination number z of the lattice is finite. Once this happens, the particle will follow its whole trajectory again: it is trapped in a closed orbit, and it does not contribute to diffusion, since the mean square displacement is bounded. The question that remains is: how serious are the closed-orbit effects? How big is the influence of taking deterministic collision rules, instead of stochastic rules? Indeed, the simulations we performed show peculiar behaviour. We will come back to this in a later section.

In previous papers we developed kinetic theory methods to deal with the stochastic Lorentz gas [9, 20]. This theory can be generalized to models with more than one type of scatterer, which is in general the case for the present chiral model. This will be done in the present paper. We also have to consider the symmetry group that corresponds to the particular scattering rules. Further, we have performed computer simulations and measured the diffusion coefficient. They will also be described in this paper. We define here the (time dependent) diffusion coefficient $D(t)$ to be proportional to the time derivative of the second moment of the distribution function for the moving particles (mean square displacement): $D(t) \equiv \frac{1}{2}\partial_t\langle x^2\rangle$. In section 8 we will comment on the validity of this definition in the case that the distribution function is not Gaussian [21, 22].

Besides a model with chiral collision rules, one can consider the mirror model [23], with scatterers that can be viewed as mirrors oriented at an angle of $\pm 45°$ with the axes. The latter will be the subject of the following paper. Another deterministic model, the so-called *alternating time model* [24], will not be considered, because this model has collision rules that depend on time (at odd/even times the scattering is over $\pm 90°$), which is a fundamentally different problem and hard to deal with theoretically.

For the chiral model the collision rules are such that the velocity is rotated: a moving particle does not scatter off a scatterer in a random direction, but in a direction that is fully determined by its direction of incidence *and* the type of scatterer: it is turned 90° clockwise or anticlockwise, or is reflected, depending on the type of scatterer. As argued before, these scattering laws cause the moving particles to be trapped in closed orbits of various lengths, of which the distribution has been investigated [26]. In the special case of the Gates model [25], where the particle always turns to the left, this results in a phase transition: for high enough scatterer density the diffusion coefficient vanishes. This is seen in the simulations. Also the present theory yields a phase transition for the Gates model. The closed orbits also imply that

phase space is split up in separate non-communicating parts, thus making ergodicity arguments inapplicable. Yet in practice one can attempt to circumvent this problem somewhat by averaging over a large enough number of different configurations of scatterers and particle trajectories. Because these problems do not arise on the level of the application of the theory, but do perhaps affect the relevance of the results, we will postpone remarks concerning these difficulties to section 8, where the theory is compared with the simulations.

We continue by giving a more detailed description of the model, also introducing some notation. A lattice site is either empty (with probability $\alpha = 1 - c$), or contains one of the three different types of scatterers: left-turners (with probability γ^{L}) right-turners (with probability γ^{R}) and reflectors (with probability β). The probabilities are normalized by

$$\alpha + \beta + \gamma^{\mathrm{L}} + \gamma^{\mathrm{R}} = 1. \tag{1.1}$$

By introducing the concentration $c = 1 - \alpha$ of occupied sites, we have also

$$\beta + \gamma^{\mathrm{L}} + \gamma^{\mathrm{R}} = c. \tag{1.2}$$

An example of a particle trajectory is shown in figure 1.

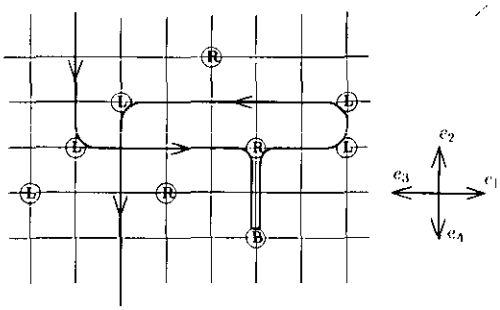

Figure 1. Chiral model with an example of a trajectory, and the basis vectors.

An interesting aspect of the chiral model is that the phase diagram of the parameters α, β, γ^{L}, γ^{R} and c is split up in separate regions ('phases') with different types of normal and abnormal diffusion. There are regions where *all* trajectories or orbits are localized to finite pieces of the lattice, or on 'perimeters' of islands [19]. In other regions the orbits extend over the macroscopic lattice. In the first type of regions diffusion does not exist, while in the other regions diffusion could exist, but does not necessarily do so, as the second moment could grow slower than linear with time. The time dependence of the mean square displacement depends strongly on the length distribution of the orbits.

Assuming, for the time being, that the model is a good model for statistical mechanics, the general phase space arguments, given in [7, 9 ,20] for the stochastic lattice Lorentz gas, apply here too. We estimated the phase space covered by the different events or particle trajectories, i.e. the order to which the events shown in figure 2 contribute. The events are classified by the order in the density c of scatterers. The difference between the stochastic model and the deterministic model enters through, for example, the orbiting collision sequences of figure 2(*c*): in a deterministic model

the particle will travel infinitely many times through this orbit, while with stochastic collision rules [9] the 'presence' of the moving particle on this trajectory decays exponentially. Apart from obvious modifications, the general formalism given in [9, 20] is assumed to be valid here too. In the next sections, we will discuss these modifications and we will calculate explicit results. We will write down the Chapman–Kolmogorov equation for this model and consider the symmetry group of the collision operators. The generalization of the Boltzmann approximation, the ring and repeated-ring approximations (and the corresponding self-consistent versions) and the full effective medium approximation (EMA) will be explained. In the final section, we present computer simulation data and compare them with these theoretical results.

2. Chapman–Kolmogorov equation

As already noted in the introduction, the chiral model is defined in two dimensions. The Chapman–Kolmogorov equation can be written down if we assign to each of the N lattice sites, labelled by $n = (n_x, n_y)$, the stochastic variables α_n, β_n, γ_n^{L} and γ_n^{R}. Of these variables, each can take on the values 0 or 1, according to the probabilities in (1.1), subject to the constraint $\alpha_n + \beta_n + \gamma_n^{\mathrm{L}} + \gamma_n^{\mathrm{R}} = 1$; thus, for given n, only one of them is different from zero. Let $p(n, i, t)$ be the probability in a given configuration of scatterers that at the integer-valued time t the moving particle is at site n and *arrives* there with 'velocity' i (i.e. comes from lattice site $n - e_i$). Here velocity variables, denoted by labels $i, j, \ldots$ ($i, j = 1, 2, 3, 4$), refer respectively to the lattice directions $e_1, e_2, e_3(= -e_1), e_4(= -e_2)$. We further use the convention that Greek labels ($\alpha, \beta = 1, 2$) denote cartesian components of two-dimensional vectors. The CK equation is then given by [27]

$$p(n + e_i, i, t + 1) = \alpha_n p(n, i, t) + \beta_n \sum_j W_{ij}^{\mathrm{B}} p(n, j, t) + \gamma_n^{\mathrm{L}} \sum_j W_{ij}^{\mathrm{L}} p(n, j, t) + \gamma_n^{\mathrm{R}} \sum_j W_{ij}^{\mathrm{R}} p(n, j, t) \tag{2.1}$$

where the transition matrices in the four-dimensional velocity space (see figure 1) are given by

$$W^{\mathrm{A}} = 1 = \begin{pmatrix} 1 & 0 & 0 & 0 \\ 0 & 1 & 0 & 0 \\ 0 & 0 & 1 & 0 \\ 0 & 0 & 0 & 1 \end{pmatrix} \qquad W^{\mathrm{B}} = \begin{pmatrix} 0 & 0 & 1 & 0 \\ 0 & 0 & 0 & 1 \\ 1 & 0 & 0 & 0 \\ 0 & 1 & 0 & 0 \end{pmatrix}$$

$$W^{\mathrm{L}} = \begin{pmatrix} 0 & 0 & 0 & 1 \\ 1 & 0 & 0 & 0 \\ 0 & 1 & 0 & 0 \\ 0 & 0 & 1 & 0 \end{pmatrix} \qquad W^{\mathrm{R}} = \begin{pmatrix} 0 & 1 & 0 & 0 \\ 0 & 0 & 1 & 0 \\ 0 & 0 & 0 & 1 \\ 1 & 0 & 0 & 0 \end{pmatrix}. \tag{2.2}$$

As expected, $(W^{\mathrm{L}})^2 = (W^{\mathrm{R}})^2 = W^{\mathrm{B}}$ and $W^{\mathrm{L}} W^{\mathrm{R}} = W^{\mathrm{R}} W^{\mathrm{L}} = 1$. The distribution function for the moving particle is $\langle p(n, i, t) \rangle$, where $\langle \ldots \rangle$ denotes the quenched average over the configuration of scatterers, i.e. an average over all $\alpha_n, \beta_n, \gamma_n^{\mathrm{L}}, \gamma_n^{\mathrm{R}}$ subject to

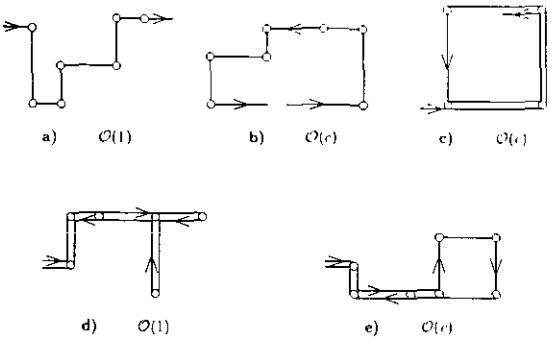

Figure 2. Examples of collision sequences that contribute to order 1 or to order c.

the constraint given above. Formally, (2.1) can be written in 4-vector and $4N$-matrix *notation [9]*:

$$p(t+1) = S^{-1}(1+K)p(t) \tag{2.3}$$

with the same streaming operator S defined as

$$S_{ni,mj} = S_{nm}\delta_{ij} = \delta_{n+e_i,m}\delta_{ij}. \tag{2.4}$$

We will often suppress the explicit notation of labels of the matrices that denote the velocity components. The collision operator K is written in the coordinate representation as

$$K_{nm} = K_n\delta_{nm} \tag{2.5}$$

where K_n is constructed from the different types of scatterers and their densities as follows:

$$K_n = \beta_n T^{\mathrm{B}} + \gamma_n^{\mathrm{L}} T^{\mathrm{L}} + \gamma_n^{\mathrm{R}} T^{\mathrm{R}} \tag{2.6}$$

where $T^X \equiv W^X - 1$, with the W defined in (2.2). This collision operator replaces $K_n = c_n T$, which is the one for the stochastic model, where c_n is the stochastic variable indicating the presence or absence of a scatterer at site n.

Now we repeat from [9, 20] the formulae that are relevant here. Performing the Laplace transform on the conditional probabilities $P(t)$, satisfying $P(0) = 1$ or $P_{ni,mj} = \delta_{ij}\delta_{nm}$, we obtain the propagator

$$\Gamma(z) = \sum_{t=1}^{\infty}(1+z)^{-t}\langle P(t)\rangle = \langle[(1+z)S - 1 - K]^{-1}\rangle \tag{2.7}$$

where the brackets also indicate the ensemble average. Later we will use the Fourier transform, which for translation invariant matrices reduces to

$$\hat{A}_{ij}(q) = \sum_n \mathrm{e}^{-\mathrm{i}qn} A_{ni,0j} \tag{2.8}$$

with the inverse transform

$$A_{ni,mj} = \frac{1}{N}\sum_{q\in 1\mathrm{BZ}} \mathrm{e}^{\mathrm{i}qn}\hat{A}_{ij}(q) \equiv \int_q \mathrm{e}^{\mathrm{i}qn}\hat{A}_{ij}(q). \tag{2.9}$$

The summation index n runs over the N lattice sites. The q are reciprocal lattice vectors, located in the first Brillouin zone (1BZ). In the thermodynamic limit ($N \to \infty$), the q sum may be replaced by an integral. The integration symbol stands for

$$\int_q (\cdots) = \int_{-\pi}^{\pi} \int_{-\pi}^{\pi} \frac{\mathrm{d}^{(2)}q}{(2\pi)^2} (\cdots). \tag{2.10}$$

The velocity autocorrelation function, which will finally lead us to the diffusion coefficient, is given by

$$\phi(t) = \frac{1}{8} \sum_{n\alpha} \sum_{ij} e_{i\alpha} e_{j\alpha} \langle P_{ni,0j}(t+1) \rangle = \frac{1}{2} \sum_{n\alpha} \langle V_\alpha | P_{n0}(t+1) | V_\alpha \rangle \tag{2.11}$$

where $\phi(0) = 1/2$. The index α labels the cartesian components of the vectors. We introduced a vector notation for the velocities, where $|V_x\rangle$ and $|V_y\rangle$ are column vectors with components $(1,0,-1,0)$ and $(0,1,0,-1)$, respectively, on the basis $\{e_1, e_2, e_3, e_4\}$ defined in figure 1. Together with $|1\rangle = (1,1,1,1)$ and $|2V_x^2 - 1\rangle = (1,-1,1,-1)$ they represent a basis of the four-dimensional velocity space. This basis diagonalizes the collision operators in the stochastic model, which have the full cubic symmetry. This is not the case for the present chiral model, as we will see later. For more details on cubic symmetric matrices we refer to [9], appendix 1.

The Green–Kubo formula for the diffusion coefficient is derived from the second moment of the probability distribution. It can equivalently be expressed in the velocity autocorrelation function (2.11). For the square lattice we have [9,22,28]

$$D = \sum_{t=0}^{\infty} \phi(t) - \tfrac{1}{4}. \tag{2.12}$$

The Laplace transform of the VACF is:

$$\Phi(z) = \sum_{t=0}^{\infty} (1+z)^{-t-1} \phi(t) = \frac{1}{8} \sum_{\alpha} \sum_{ij} e_{i\alpha} \langle \hat{\Gamma}_{ij}(0,z) \rangle e_{j\alpha} = \frac{1}{2} \sum_{\alpha} \langle V_\alpha | \hat{\Gamma}(0,z) | V_\alpha \rangle. \tag{2.13}$$

The static diffusion coefficient is then readily written as:

$$D = \Phi(z=0) - \tfrac{1}{4}. \tag{2.14}$$

This will be the quantity that we will calculate in this paper for the chiral model. In previous papers we described several approximation schemes that try to deal with the disorder represented by the stochastic matrix K_{nm}. We will generalize them here. The basic ingredient is the *ring integral* or ring matrix, which is essentially the probability of return of the moving particle to a site it has already visited before. Returns ('rings') introduce correlations between collisions, and are thus to be considered as corrections to the results given by the Boltzmann equation. The ring integral is written as

$$R(z) \equiv G_{00}(z) = \int_q \hat{G}(q,z) = \int_q \left[(1+z) \mathrm{e}^{\mathrm{i}qV} - 1 - K'(z) \right]^{-1} \tag{2.15}$$

Here, G denotes the propagator in some approximation where the disorder is smoothed out and we have a uniform system. $\hat{G}(q,z)$ is its Fourier transform (2.8) and $\exp(iqV)$ is the Fourier transform of the free streaming operator S of (2.4), see (2.8). We will consider several approximations, which also affect the form of the collision operator, and may induce a frequency dependence. For this reason we denoted it as $K'(z)$. The ring integral will be studied in detail in section 7. Later we will discuss the approximations in more detail, but it is convenient to first introduce a basis of velocity space that diagonalizes the collision operator K, and thereby all the other operators.

3. Symmetries

For the subsequent analysis it is convenient to diagonalize the matrices of the operators we need. The basis on which this happens is related to the symmetry of the matrices we use. Using the matrices (2.2) which form a basis, any general rotation-symmetric matrix can be written as

$$H = a1 + bW^{\mathrm{B}} + c^{\mathrm{L}}W^{\mathrm{L}} + c^{\mathrm{R}}W^{\mathrm{R}}. \tag{3.1}$$

Using the representation introduced below (2.11), one can easily verify that $|V_x\rangle$ and $|V_y\rangle$ are not eigenvectors of H. This reflects the difference with the full cubic symmetry of the stochastic model. However, as the matrices in (2.2) commute, we still can find a set of eigenvectors that span the velocity space, i.e. we can diagonalize the general matrix H. One can verify that this is realized by choosing the basis $\{|V_+\rangle, |V_-\rangle\}$, which is expressed in $\{|V_x\rangle, |V_y\rangle\}$ as

$$|V_+\rangle = |V_x\rangle + \mathrm{i}|V_y\rangle \qquad |V_+\rangle = |V_x\rangle - \mathrm{i}|V_y\rangle. \tag{3.2}$$

where $|V_x\rangle$ and $|V_y\rangle$ are defined below (2.11). Next we introduce eigenvectors

$$|\psi_o\rangle = |1\rangle \qquad |\psi_1\rangle = |V_+\rangle \qquad |\psi_2\rangle = |V_-\rangle \qquad |\psi_3\rangle = |V_x^2 - V_y^2\rangle \tag{3.3}$$

which are normalized with respect to the (Hermitian) inner product

$$\langle a(V)|b(V)\rangle \equiv \frac{1}{4}\sum_i a^*(e_i)b(e_i). \tag{3.4}$$

The eigenvalues of (3.1) corresponding to (3.3) are:

$$\begin{aligned} h_0 &= a + b + c^{\mathrm{L}} + c^{\mathrm{R}} \\ h_1 &= h_+ = a - b - \mathrm{i}c^{\mathrm{L}} + \mathrm{i}c^{\mathrm{R}} \\ h_2 &= h_- = a - b + \mathrm{i}c^{\mathrm{L}} - \mathrm{i}c^{\mathrm{R}} \\ h_3 &= a + b - c^{\mathrm{L}} - c^{\mathrm{R}}. \end{aligned} \tag{3.5}$$

Using this, the collision operators $T^{\mathcal{X}} \equiv W^{\mathcal{X}} - 1$ are seen to have the following eigenvalues (see (2.2)):

$$\begin{array}{lll} t_1^{\mathrm{B}} = -2 & t_1^{\mathrm{L}} = -1 - \mathrm{i} & t_1^{\mathrm{R}} = -1 + \mathrm{i} \\ t_2^{\mathrm{B}} = -2 & t_2^{\mathrm{L}} = -1 + \mathrm{i} & t_2^{\mathrm{R}} = -1 - \mathrm{i} \\ t_3^{\mathrm{B}} = \ \ 0 & t_3^{\mathrm{L}} = -2 & t_3^{\mathrm{R}} = -2. \end{array} \tag{3.6}$$

Using this basis of eigenvectors, the propagator (2.7) and the ring operator (2.15) are diagonalized, and the expression for the diffusion coefficient (essentially the $z = 0$ value of the Laplace transform of the VACF) is given by:

$$D = \frac{1}{4}\sum_{\ell=1}^{2}\langle\psi_\ell|\hat{\Gamma}(q=0,z=0)|\psi_\ell\rangle - \tfrac{1}{4} = \tfrac{1}{4}(\lambda_+^{-1} + \lambda_-^{-1} - 1) \tag{3.7}$$

Γ is the Fourier transform of the propagator (2.7). We recall that the brackets also imply an average over the randomness present in the stochastic matrix K. After appropriate averaging, the (vector) eigenvalues of an effective (translation symmetric) collision matrix K are $-\lambda_1 = -\lambda_+$ and $-\lambda_2 = -\lambda_-$. In the next sections we will discuss several ways of approximating these eigenvalues and thus the value for the diffusion coefficient.

4. Boltzmann approximation

The most straightforward approximation is to assume molecular chaos [9]. This means that we do not account for any correlation between the collisions of the moving particle with scatterers. It is equivalent to deciding whether there is a scatterer every time a site is encountered, using the probabilities α, β, γ^{L} and γ^{R}.

Explicitly, we will have for the collision operator, occurring in (2.7), for *every* site n:

$$K^0 = \langle K\rangle = \beta T^{\mathrm{B}} + \gamma^{\mathrm{L}} T^{\mathrm{L}} + \gamma^{\mathrm{R}} T^{\mathrm{R}}. \tag{4.1}$$

The eigenvalues λ_+ and λ_- are seen to be:

$$\lambda_+ = \lambda_-^* = -\beta t_1^{\mathrm{B}} - \gamma^{\mathrm{L}} t_1^{\mathrm{L}} - \gamma^{\mathrm{R}} t_1^{\mathrm{R}} = 2\beta + \gamma^{\mathrm{L}} + \gamma^{\mathrm{R}} + \mathrm{i}(\gamma^{\mathrm{L}} - \gamma^{\mathrm{R}}). \tag{4.2}$$

For the diffusion coefficient (3.7) we need twice the real part of λ_+^{-1}, yielding

$$D^0 = \frac{1}{4}\,\frac{2\beta + \gamma^{\mathrm{L}} + \gamma^{\mathrm{R}}}{2\beta^2 + 2\beta(\gamma^{\mathrm{L}} + \gamma^{\mathrm{R}}) + {\gamma^{\mathrm{L}}}^2 + {\gamma^{\mathrm{R}}}^2} - \frac{1}{4}. \tag{4.3}$$

Recall that the probability α occurs here implicitly through the normalization (1.1). For the case ($\beta = 0$, $\gamma^{\mathrm{R}} = \gamma^{\mathrm{L}} = \frac{1}{2}c$) this yields $D^0 = \frac{1}{2}c - \frac{1}{4}$, which is the same as for the Boltzmann approximation for the stochastic model with only deflections, and the Ruijgrok–Cohen model with equal amounts of right- and left-oriented mirrors [23].

Using the Boltzmann propagator G^0, i.e. (2.7) with K replaced by K^0, we can write down a *systematic* expansion of the exact propagator Γ in terms of Boltzmann propagators G^0. In [20] we discussed that the Dyson equation

$$\Gamma = G^0 + G^0 B\Gamma = (G^{0\,-1} - B)^{-1} \tag{4.4}$$

generates all terms in such an expansion. In this equation, B denotes the set of collision (or self-energy) diagrams, which account for correlations. In the Boltzmann approximation, the higher-order terms vanish, i.e. $B = 0$, leaving G^0. In the following we discuss several approximations that resum subsets of the self-energy diagrams.

5. Ring and repeated-ring approximation

A ring event corresponds to a return of the moving particle to a site it has already visited before. This site can be empty, or it can be occupied by a scatterer. For the chiral model, we further have to distinguish between different types of scatterers that can be at the site. In a quenched configuration of scatterers, the particle will, of course, upon return to the same site, encounter the same scatterer it hit before. A repeated-ring collision sequence will thus be one of

$$T^{\mathrm{B}}(RT^{\mathrm{B}})^{\ell} \qquad T^{\mathrm{L}}(RT^{\mathrm{L}})^{\ell} \qquad T^{\mathrm{R}}(RT^{\mathrm{R}})^{\ell} \tag{5.1}$$

with $\ell = 0, 1, 2, \ldots$, and *not*, for instance

$$T^{\mathrm{B}}\,RT^{\mathrm{L}}\,RT^{\mathrm{L}}\,RT^{\mathrm{R}}\,RT^{\mathrm{B}}\,RT^{\mathrm{R}}\,RT^{\mathrm{B}}\,RT^{\mathrm{L}}.$$

R is the ring operator, cf (2.15). Accordingly, the ring approximation (RA) is given by [20] $K_{RA} = K^0 + B_{RA}$ with

$$B_{RA} = \beta T^{\mathrm{B}} R^0 T^{\mathrm{B}} + \gamma^{\mathrm{L}} T^{\mathrm{L}} R^0 T^{\mathrm{L}} + \gamma^{\mathrm{R}} T^{\mathrm{R}} R^0 T^{\mathrm{R}}. \tag{5.2}$$

Here $R^0 = R^0(z)$ the *simple ring integral* of the Boltzmann propagator, i.e. (2.15) with $K'(z)$ replaced by K^0 of (4.1). The ring integral is calculated in section 7. Analogously, the repeated-ring approximation (RRA), accounting for infinitely many returns, is written as

$$\begin{aligned} B_{\mathrm{RRA}} &= \beta\left(T^{\mathrm{B}}R^0T^{\mathrm{B}} + T^{\mathrm{B}}(R^0T^{\mathrm{B}})^2 + T^{\mathrm{B}}(R^0T^{\mathrm{B}})^3 + \cdots\right) \\ &\quad + \gamma^{\mathrm{L}}\left(T^{\mathrm{L}}R^0T^{\mathrm{L}} + T^{\mathrm{L}}(R^0T^{\mathrm{L}})^2 + T^{\mathrm{L}}(R^0T^{\mathrm{L}})^3 + \cdots\right) \\ &\quad + \gamma^{\mathrm{R}}\left(T^{\mathrm{R}}R^0T^{\mathrm{R}} + T^{\mathrm{R}}(R^0T^{\mathrm{R}})^2 + T^{\mathrm{R}}(R^0T^{\mathrm{R}})^3 + \cdots\right) \\ &= \beta T^{\mathrm{B}}R^0T^{\mathrm{B}}(1 - R^0T^{\mathrm{B}})^{-1} + \\ &\quad \gamma^{\mathrm{L}}T^{\mathrm{L}}R^0T^{\mathrm{L}}(1 - R^0T^{\mathrm{L}})^{-1} + \gamma^{\mathrm{R}}T^{\mathrm{R}}R^0T^{\mathrm{R}}(1 - R^0T^{\mathrm{R}})^{-1}. \end{aligned} \tag{5.3}$$

Here it is in order to remark that in the chiral model there are at most four (the coordination number) returns possible with intermediate uncorrelated collision sequences. Every return after this results in orbiting collision sequences such as depicted in figure 2(*c*). We will come back to this point in the discussion, where for a specific model we look at the difference between a finite number of returns and infinitely many returns.

The self-consistent ring and repeated-ring formulations (SRA and SRRA, respectively) are straightforwardly obtained using an iteration procedure: the ring integral R^0 is replaced by $R(z)$, i.e. the ring integral over an effective propagator with an effective collision operator $K^{\mathrm{e}} = cT^{\mathrm{e}} = K^0 + B$. Here, B is given for the SRA and SRRA in (5.2) and (5.3), respectively, with $R^0(z) \to R(z)$. So the collision operator depends on the ring integral. We write the effective collision operator in the form $cT^{\mathrm{e}}(z)$ (with c the density of scatterers, irrespective of the type) to remain in contact with the notation in [9, 20]. The $z = 0$ value will be needed for the diffusion coefficient.

Note that for the chiral model we do not have an exact solution for the case that the lattice is completely filled with scatterers. The reason is that it does not reduce to a standard (correlated) random walk, as we still have the disorder of *different* scatterers. Consequently, we *cannot* write down the high-density equivalent of the ring and repeated-ring approximations. The stochastic Lorentz gas of [9, 20] has only one type of scatterer, so the filled lattice has no disorder and an exact solution can be obtained.

6. Effective medium approximation

Finally, we discuss the application to this model of the effective medium approximation, which has proved to be successful in the theory of random resistor networks [29] and hopping models [30–34]. The approximation can be obtained by resumming the returns to the same site using an effective propagator to account for a uniform effective medium, followed by the requirement of a vanishing first-order correction in a perturbation expansion in terms of this effective medium propagator. This requirement determines the effective collision operator. In [20] we analysed which subset of diagrams out of the set of collision diagrams of the exact expansion are accounted for by this approximation. In summary, the EMA is such that it accounts for all correlations which refer to the same site (ring-type correlations), followed by nesting of these repeated-ring diagrams. The weights are such that the description is in itself consistent. Events that are definitely *not* accounted for refer to crossing events between scatterers at different sites. The effective medium approximation having the characteristics of a ring approximation means that the application to the chiral model is only more complicated in the sense that we have different types of scatterers: we have to sum four terms. The effective medium condition is [9, 20]

$$\left\langle \frac{K_n - cT^{\mathrm{e}}}{1 - R(K_n - cT^{\mathrm{e}})} \right\rangle = 0 \tag{6.1}$$

where the collision operator is now of the form (2.6), and $cT^{\mathrm{e}} = K^{\mathrm{e}}$ is the effective operator (see end of preceding section). The brackets indicate an average over the scatterer configuration, here only for one site. Using the probabilities with which the different scatterers occur, we can write the *EMA condition* for the chiral model explicitly as

$$\alpha \frac{-cT^{\mathrm{e}}}{1 - R(-cT^{\mathrm{e}})} + \beta \frac{T^{\mathrm{B}} - cT^{\mathrm{e}}}{1 - R(T^{\mathrm{B}} - cT^{\mathrm{e}})} + \gamma^{\mathrm{L}} \frac{T^{\mathrm{L}} - cT^{\mathrm{e}}}{1 - R(T^{\mathrm{L}} - cT^{\mathrm{e}})} + \gamma^{\mathrm{R}} \frac{T^{\mathrm{R}} - cT^{\mathrm{e}}}{1 - R(T^{\mathrm{R}} - cT^{\mathrm{e}})} = 0. \tag{6.2}$$

Here, R is the ring operator for the effective medium (calculated in section 7), accounting for returns of the moving particle to the same scatterer after travelling through an 'effective mixture' of scatterers and empty sites. In this effective mixture, the collisions with the scatterers (and 'virtual collisions' with empty sites) are assumed to be uncorrelated. Note that the probabilities α, β, γ^{L} and γ^{R}, occurring in (6.2), are normalized by (1.1). Corrections to the EMA [9, 20] involve 'crossings' between two different sites, i.e. non-ring diagrams, which are far more complicated to incorporate in the theory [35–37]. Intuitively the EMA accounts for the nested ring diagrams in the same way as it does in the stochastic case. Also here it is possible, using a diagrammatic analysis (cf [20]), to determine the weights that the nested ring diagrams obtain. However, we did not do this. The EMA equation we obtain here for the chiral model is not as easily solved as the EMA equation for the stochastic model. To explain this we first note that, due to the diagonalization (see section 3), (6.2) can readily be seen to be the equation for the *eigenvalues* of the effective collision operator. For every eigenvalue, (6.2) contains four terms. In general this leaves a fourth-order equation to solve. Only in some special cases, like the Gates model ($\beta = \gamma^{\mathrm{L}} = 0$, *or* $\beta = \gamma^{\mathrm{R}} = 0$), do simplifications occur. An additional difficulty is that the eigenvalues are complex numbers, expressing the chiral properties of the scatterers.

The different approximations discussed in this and preceding sections are obtained by making specific choices for the collision operator, which we will denote by Λ, having eigenvalues λ_ℓ. As we have diagonalized the matrices, the operator expressions (5.2), (5.3) and (6.2) directly yield the expressions for λ_ℓ in terms of the eigenvalues of the collision operators T^{L}, T^{R} and T^{B}, and the ring integral R. For the EMA we have to solve the coupled equations (7.10) and (6.2), where the latter yields the eigenvalues λ_ℓ of $\Lambda = -cT^{\mathrm{e}}$, that can be substituted in (7.10) to calculate the corresponding eigenvalues of the ring operator.

The diffusion coefficient (3.7) can be calculated using the $z = 0$ values of the vector eigenvalues $t_1^{\mathrm{e}} = -\lambda_1/c = -\lambda_+/c$ and $t_2^{\mathrm{e}} = -\lambda_2/c = -\lambda_-/c$ of the effective collision operator T^{e}. The values for the $\lambda_\pm$ depend on the approximation used: Boltzmann, (self-consistent) ring or repeated-ring approximation, or EMA.

Finally, we note that effective densities of the different types of scatterers can be calculated from the final (eigen)values ct_ℓ^{e} of cT^{e}, in any of the approximations. From the matrix equation

$$cT^{\mathrm{e}} = \beta^{\mathrm{e}} T^{\mathrm{B}} + \gamma^{\mathrm{L}^{\mathrm{e}}} T^{\mathrm{L}} + \gamma^{\mathrm{R}^{\mathrm{e}}} T^{\mathrm{R}} \tag{6.3}$$

we obtain

$$\begin{aligned} \beta^{\mathrm{e}} &= -\tfrac{1}{4}c(t_1^{\mathrm{e}} + t_2^{\mathrm{e}} - t_3^{\mathrm{e}}) \\ \gamma^{\mathrm{L}^{\mathrm{e}}} &= \tfrac{1}{4}c(\mathrm{i}(t_1^{\mathrm{e}} - t_2^{\mathrm{e}}) - t_3^{\mathrm{e}}) \\ \gamma^{\mathrm{R}^{\mathrm{e}}} &= \tfrac{1}{4}c(-\mathrm{i}(t_1^{\mathrm{e}} - t_2^{\mathrm{e}}) - t_3^{\mathrm{e}}). \end{aligned} \tag{6.4}$$

7. Ring integral

For the calculation of the transition probabilities, (i.e. the effective densities of the different scatterers) in the various approximations, we restrict ourselves to the $z = 0$ case, as we aim for the static diffusion coefficient. We evaluate the eigenvalues of the ring operator R, given by the integral (2.15):

$$r_\ell = \langle \psi_\ell | R | \psi_\ell \rangle = \int_q \langle \psi_\ell | A_\ell \rangle \tag{7.1}$$

with A_ℓ satisfying

$$\left(\mathrm{e}^{\mathrm{i}qV} - 1 - cT^{\mathrm{e}}\right) |A_\ell\rangle = |\psi_\ell\rangle. \tag{7.2}$$

We define the matrix elements [9] $B_{\ell\ell'}$ by

$$B_{\ell'\ell} = \left\langle \psi_{\ell'} \right| \left(\mathrm{e}^{\mathrm{i}qV} - 1\right)^{-1} \left| \psi_\ell \right\rangle \tag{7.3}$$

and we decompose the effective collision matrix $-cT^{\mathrm{e}} = \Lambda$ into projection operators P_ℓ on the eigenspaces (3.3) of the rotation symmetric operator:

$$-cT^{\mathrm{e}} = \Lambda = \lambda_1 P_1 + \lambda_2 P_2 + \lambda_3 P_3 \tag{7.4}$$

where

$$P_\ell = |\psi_\ell\rangle\langle\psi_\ell|. \tag{7.5}$$

The values or expressions that we will substitute for the λ will correspond to the actual approximation (RA, RRA, SRA, SRRA or EMA) that we wish to study. The equations for the components of the vector A are then

$$\begin{pmatrix} 1+\lambda_1 B_{11} & \lambda_2 B_{12} & \lambda_3 B_{13} \\ \lambda_1 B_{21} & 1+\lambda_2 B_{22} & \lambda_3 B_{23} \\ \lambda_1 B_{31} & \lambda_2 B_{32} & 1+\lambda_3 B_{33} \end{pmatrix} \begin{pmatrix} \langle\psi_1|A_\ell\rangle \\ \langle\psi_2|A_\ell\rangle \\ \langle\psi_3|A_\ell\rangle \end{pmatrix} = \begin{pmatrix} B_{1\ell} \\ B_{2\ell} \\ B_{3\ell} \end{pmatrix}. \tag{7.6}$$

The matrix elements $B_{\ell'\ell}$ are given by:

$$\begin{aligned} &B_{11} = B_{22} = B_{33} = -\tfrac{1}{2} && B_{12} = B_{21} = 0 \\ &B_{13} = -B_{31}^* = -ih_x + h_y && B_{23} = -B_{32}^* = -ih_x - h_y \end{aligned} \tag{7.7}$$

with $h_\alpha \equiv \frac{1}{4}\sin q_\alpha/(1-\cos q_\alpha)$. The $\langle\psi_{\ell'}|A_\ell\rangle$ can now be calculated. Defining $f_\alpha^2 = 2h_\alpha^2$, and after some algebra, the result can be written in the form

$$r_\ell = \int_q \frac{A_\ell + 8B_\ell(f_x^2+f_y^2)}{E+8F(f_x^2+f_y^2)} \tag{7.8}$$

for $\ell = 1,2,3$. The coefficients A_ℓ, B_ℓ, E and F are given by:

$$\begin{aligned} &A_1 = -\tfrac{1}{2}(1-\tfrac{1}{2}\lambda_2)(1-\tfrac{1}{2}\lambda_3) && B_1 = \tfrac{1}{16}\lambda_3(1-\lambda_2) \\ &A_2 = -\tfrac{1}{2}(1-\tfrac{1}{2}\lambda_1)(1-\tfrac{1}{2}\lambda_3) && B_2 = \tfrac{1}{16}\lambda_3(1-\lambda_1) \\ &A_3 = -\tfrac{1}{2}(1-\tfrac{1}{2}\lambda_1)(1-\tfrac{1}{2}\lambda_2) && B_3 = \tfrac{1}{16}(\lambda_1+\lambda_2-\lambda_1\lambda_2) \\ &E = (1-\tfrac{1}{2}\lambda_1)(1-\tfrac{1}{2}\lambda_2)(1-\tfrac{1}{2}\lambda_3) && F = \tfrac{1}{16}\lambda_3(\lambda_1+\lambda_2-\lambda_1\lambda_2). \end{aligned} \tag{7.9}$$

This integral has been calculated analytically in [9], appendix 2. We repeat the result

$$r_\ell(\lambda_1,\lambda_2,\lambda_3) = \frac{A_\ell - 2B_\ell}{E-2F} + \frac{B_\ell E - A_\ell F}{(E-2F)F} J \tag{7.10}$$

with

$$J = \begin{cases} \delta[1+(2/\pi)\tan^{-1}\frac{1}{2}(\delta^{-1}-\delta)] & \text{for } \delta^2 > 0 \\ \frac{2}{\pi}\eta\ln(\eta+1)/(\eta-1) & \text{for } \delta^2 = -\eta^2 < 0. \end{cases} \tag{7.11}$$

The quantity δ is defined by $\delta^2 = F/(E-F)$. We note, from the fact that λ_1 and λ_2 are complex conjugate, we have that E and F are real numbers, and A_1 and B_1 are the complex conjugates of A_2 and B_2, respectively. The consequence is that r_1 and r_2 are complex conjugate and consequently the next values of λ_1 and λ_2 in an iteration procedure (for a self-consistent evaluation). This will give a real number for the diffusion coefficient, as one would expect. As a check of the expressions obtained here, we can set λ_1 equal to λ_2 in (7.9), i.e. assuming degeneracy of the vector eigenvalue. This, expectedly, leads to the same expression as obtained in [9], where the vector eigenvalue is degenerate.

8. Results and discussion

The kinetic theory that was developed for the stochastic lattice Lorentz gas (see [9, 20]), has been applied to the chiral model, which is deterministic and has chiral collision rules. Here we evaluate the static diffusion coefficient. For an investigation of the time dependence of the diffusion coefficient and velocity autocorrelation function (VACF) in, for instance, the EMA, we refer to [33, 34]; for the stochastic lattice Lorentz gas the long-time tails for the VACF were analysed in [41]. Explicit results for the effective medium approximation can be obtained by using numerical techniques for carrying out the iteration procedure prescribed by the coupled set of equations (6.2) and (7.10). As we are looking for the static properties, we restrict ourselves to the $z = 0$ case, corresponding to $t \to \infty$. The procedure is more involved than for the stochastic model. For the latter, the problem reduces to the search for fixed points in a mapping of the two-dimensional parameter space $\{\lambda_v, \lambda_t\}$ onto itself, where λ_v and λ_t are the eigenvalues for the vector and tensor eigenspaces [9]. In the present case, we have *three* independent parameters: the complex conjugate λ_1 and λ_2, and a real number λ_3 (see section 7). One could imagine that the structure of the function in this parameter space, which we do not know *a priori*, is not necessarily such that one will indeed find relevant fixed points. Moreover, the EMA equation (6.2) (to be solved at every intermediate iteration step) has four terms, as we distinguish between empty sites and three types of scatterers. Consequently, the equation for the eigenvalues λ_ℓ will in general be fourth order, and it might be a problem to find the physically relevant branch of the solution. For these reasons, it is not very likely that we will find solutions for *every* choice of parameters.

In order to find the physically relevant branch of the solutions, one should obviously choose the correct starting values. For the stochastic model, the outcome was insensitive to whether we take the Boltzmann value or a value that is a factor five different from it. To attack problems of convergence for the present case, we also take advantage of the knowledge of the result of a slightly different c value; that is, while performing the calculations for a sequence of increasing c values, one could start the iterations for a certain c with a previous result. Unfortunately, even this does not guarantee solutions for some parameter choices. For example, the set $(\beta = \gamma^L = \gamma^R = \frac{1}{3}c)$ or sets with larger β values do not seem to yield convergence, neither in the EMA nor in the other self-consistent approximations SRA and SRRA. For the case $(\beta = 0.33c, \gamma^L = \gamma^R = 0.335c)$ convergence is still obtained. The results for $cD(c)$, however, are of the order of 0.1, which is rather small, as compared with the other models we will discuss later. This may indicate that the threshold value β_c above which no diffusion exists, is actually lower than the theoretical upper bound [19] given by the two-dimensional site percolation threshold: $\beta = c_p = 0.41$. Obviously, the explanation for this is that chiral scatterers may block an area.

In the following we present the results for some typical parameter sets for which we *were* able to obtain results. Note that the ring and repeated-ring approximation (and of course the Boltzmann approximation) are straightforward calculations, which can be carried out for any set of parameters.

For some models, we also performed computer simulations, using typically several thousands of moving particles moving in a lattice of size up to 1000×1000 sites, a fraction of which was randomly filled with scatterers.

8.1. The Gates model

A special case of the chiral model is the Gates model [25]. It consists of randomly placed scatterers of *only one type*: either left-turners *or* right-turners. This model clearly shows a phase transition from extended to localized orbits or trajectories when the model parameters are varied: at a high enough density of scatterers, the moving particles can not diffuse away, and will soon be trapped in closed orbits. The mean square displacement is thus finite, and diffusion does not exist. This property of the model, caused by the chiral nature of the scatterers, is not reproduced by the Boltzmann equation, as it is strongly related to correlations between collisions. Indeed, as one can verify from (4.3), the Boltzmann diffusion coefficient goes to zero only in the high-density limit.

For the Gates model we calculated the diffusion coefficient in all approximations derived in this paper. The fact that there is only one type of scatterer facilitates the computation of the EMA values, for the EMA equation (6.2) is only a quadratic equation instead of a quartic. For this model the low-density Boltzmann result is not modified, because there are no direct reflections (i.e. $\beta = 0$).

In figure 3 we plotted the results of the approximations, together with computer simulations for the (time-dependent) diffusion coefficient at the indicated times. From the figure it is clear that the asymptotic time range has probably not yet been reached; later we will comment further on this phenomenon. The EMA shows a phase transition at $\gamma = c \simeq 0.67$. The ring approximation (RA) also shows a phase transition, while the repeated-ring approximation (RRA) is even worse than the Boltzmann approximation. At this point it is interesting to come back to the earlier remark that one can return at most four times to the same scatterer with intermediate uncorrelated collisions. As we have a considerable discrepancy between the ring approximation and the repeated-ring approximation, the question arises what an m-times-repeated ring approximation would give, i.e. substituting the collision operators by $T + TR^0T + \cdots + T(R^0T)^m$, where T stands for T^{L} or T^{R}. The results are displayed in figure 4. They show that apparently the successive summation of more and more terms does not converge in a decent way. There may exist large differences between the approximations with different values of ℓ. Only for very large m (200 or 300) the result coincides with that obtained with the expression $T(1 - RT)^{-1}$, *but only up to* $c = \gamma \simeq 0.69$. Apparently the expression for the infinite sum exceeds the radius of convergence of the series. In some way the EMA resums all these diagrams with weights that are such that the divergences of individual terms are suppressed and the qualitative feature of the transition is recovered. This is completely in the spirit of our analysis in [20].

The self-consistent calculations for the Gates model seem to fall off too quickly to describe the simulations. Similar results were obtained before in [20]. No substantial difference was observed here upon taking a finite number of rings as described above.

It seems that here also, out of the collection of approximations, the EMA is the best one; this is in accordance with what we found in [9, 20]. Also in agreement with the results of [20] is the fact that the self-consistent ring type curves bend off strongly from the EMA and become unsolvable very soon, i.e. at rather low density.

In the simulations for the Gates model, plotted in figure 3, we extracted the diffusion coefficient from runs with different numbers of time steps. For more extensive simulations we refer to [26]. There it is found that the transition from extended to localized orbits is at $c = \gamma \simeq 0.51$, where γ stands for either γ^{R} or γ^{L}, by symmetry. However, as we see in figure 3, it may be such that even below this critical concentra-

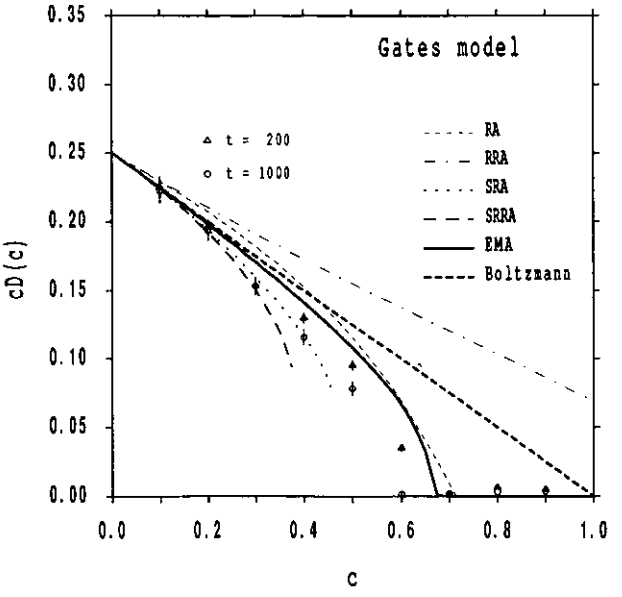

Figure 3. Various approximations for the Gates model, together with simulations. Simulation results for several values of time t.

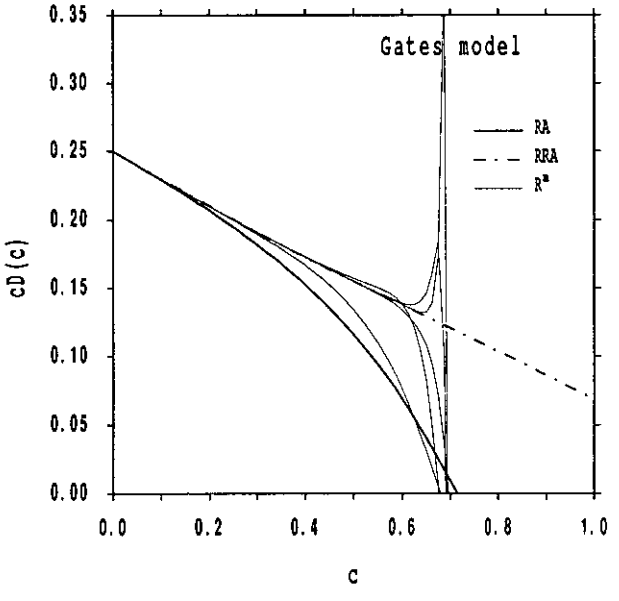

Figure 4. Comparison of repeated-ring approximations for the Gates model, $m = 2, 4, 8, 12, 16, 20$.

tion diffusion is not well defined: the $t = 1000$ simulation data lie below the $t = 200$ simulation data. The diffusion coefficient is calculated from the slope of the mean square displacement. In [26] even more peculiar behaviour is reported, namely that the diffusion coefficient (measured at a certain time t, as the mean square displacement is not really linear) is larger for $\gamma = c \simeq 0.48$ than for $\gamma = c \simeq 0.45$. However, if we naively restrict ourselves to the results from rather short simulations, the present work

is in qualitative agreement with the experiments. The discrepancy of the prediction of the threshold ($\gamma = 0.67$), with respect to the numerical results, is comparable to the prediction of the percolation threshold for the three-dimensional bond percolation model by the original EMA theory: $c_p = \frac{2}{3}$, as compared with simulation results that indicate $c_p \simeq 0.75$ [29, 34, 37].

8.2. Other models

More challenging calculations for the chiral model are those that include more types of scatterers. The first case we will discuss is that with left- and right-turners, but no backscatterers, i.e. we take $\beta = 0$. In the past, this version has received attention in numerical studies of critical exponents [38, 39]. The model with $\gamma^L = \gamma^R = \frac{1}{2}c$ has the same Boltzmann approximation for the diffusion coefficient as the stochastic model [9] with $\gamma = \frac{1}{2}$. The EMA, and also the ring and repeated-ring approximation, are about the same as the Boltzmann approximation. We stress that this statement holds for the vectorial eigenvalues $\lambda_\pm$ and $r_\pm$ entering in the VACF, but not necessarily for the tensor eigenvalues λ_3 and r_3 (see also [9]); the latter do not enter directly into the diffusion coefficient, but do play a role in the iteration of the equations for the SRA, SRRA and EMA.

The results are plotted in figure 5, together with some simulations. For low densities we have agreement, but for higher densities we find peculiar behaviour. If we calculate the diffusion coefficient from the slope of the mean square displacement at a longer time, we get a result that is lower than that obtained for shorter times. This is most prominent at densities of 0.7 to 0.8, but also for lower densities we find systematic deviations. This serves as an argument to critically examine the existence of diffusion for this model, defined through the second moment of the probability distribution [22]. To investigate this question in more detail, one could look at the kurtosis, which is defined as [40]

$$K = \frac{\langle x^4 \rangle - 3\langle x^2 \rangle^2}{\langle x^2 \rangle^2}. \tag{8.1}$$

If the probability distribution for the moving particles is Gaussian, the second moment exists, and the kurtosis vanishes. Simulations carried out for the chiral model, however, show a kurtosis that increases from zero at low densities to values of order one for high densities, as we show in figure 6. A similar dependence of the kurtosis on the density of scatterers was found for the mirror model [21, 22]. The deviation of the radial probability distribution from a Gaussian form is argued to come from the contribution of relatively short closed orbits. We did not investigate the behaviour of higher moments.

Regarding these deviations from the Gaussian form, some remarks can be made concerning the definition of diffusion. From the usual diffusion equation, Fick's law, follows that the probability distribution has the Gaussian form, thus giving the dependence on time of all the moments of the distribution. The second moment then grows linearly with time, with a proportionality coefficient that is defined as the diffusion coefficient. However, if the dynamics can not be described by a Markov process, it may be different. It could be that the second moment grows linearly with time, thus allowing the choice of a proportionality coefficient, but that the higher moments do not satisfy the form of a Gaussian distribution. It then becomes questionable, from some point of view, if one should use the term 'diffusion' at all. In the present paper,

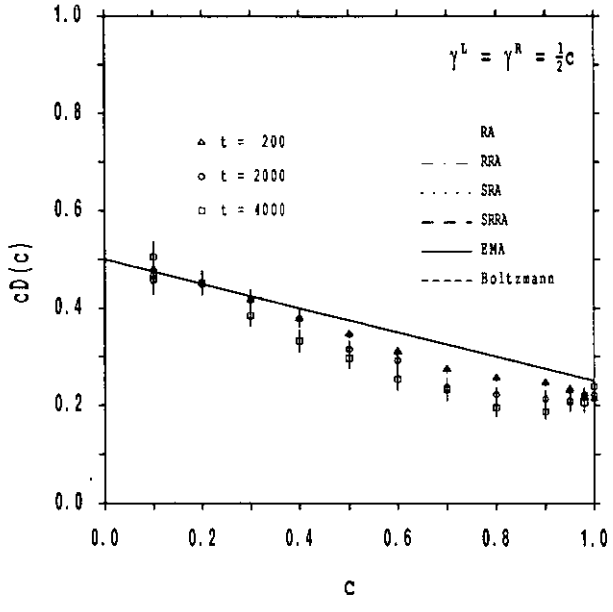

Figure 5. Chiral model for $\beta = 0$ and $\gamma^L = \gamma^R = \frac{1}{2}c$. Simulation results for several values of time t.

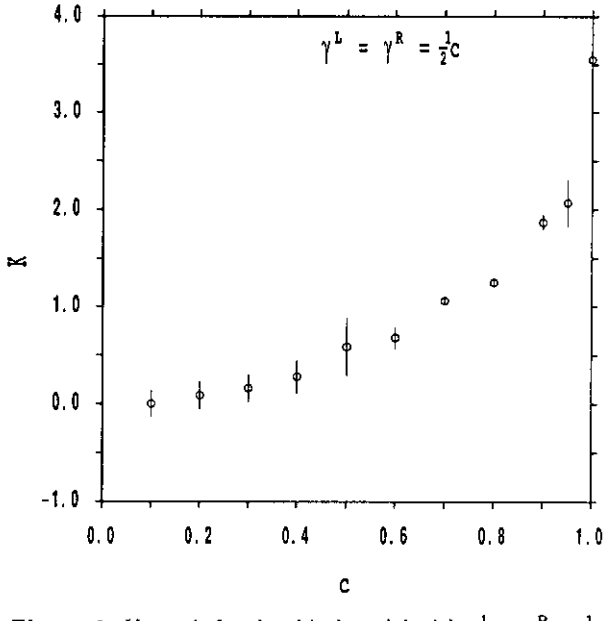

Figure 6. Kurtosis for the chiral model with $\gamma^L = \gamma^R = \frac{1}{2}c$.

however, we conveniently define the (time dependent) diffusion coefficient $D(t)$ to be proportional to the time derivative of the second moment or mean square displacement: $D(t) \equiv \frac{1}{2}\partial_t\langle x^2\rangle$.

For the case that there is an excess of left- or right-turners ($\gamma^L \neq \gamma^R$), the EMA predicts a phase transition, even if the densities differ only slightly from $\frac{1}{2}c$. This is seen in figure 7 for a typical set of parameters. These findings are in agreement with

the phase diagram of the chiral model where the complete phase space of parameters α, β,γ^{L}, γ^{R} and c is studied [22, 26]. However, also this transition is only a qualitative result: simulations show a threshold that is lower than the EMA threshold. Again, it seems that simulating longer times yields lower results for the diffusion coefficient.

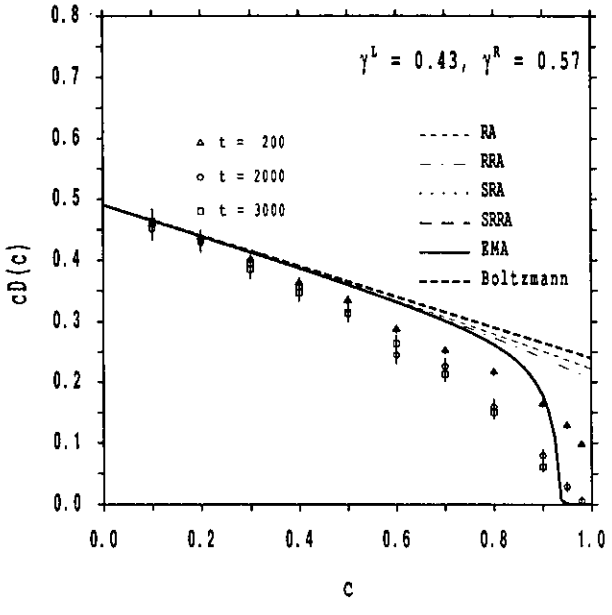

Figure 7. Chiral model with $\beta = 0$ and $\gamma^{\mathrm{L}} \neq \gamma^{\mathrm{R}}$. Note: SRA and SRRA, only up to $c \simeq 0.4$, are hidden in other curves. Simulation results for several values of time t.

Finally, we present some results for the case when the density β of backscatterers is non-zero. According to [19, 26], the simulations refer to a region of extended orbits in the 'phase diagram' of the parameters $\{\alpha, \beta\}$. There diffusion may occur. Some cases are presented in figure 8, where one can see that the EMA for these models yields a rather unexpected result: for larger densities c, the EMA diffusion coefficient is *higher* than the values (4.3) predicted by the Boltzmann equation. For short times ($t = 200$) and low densities of scatterers, the simulations more or less agree with the EMA, and deviate significantly from Boltzmann, confirming our expectation that the Boltzmann equation breaks down in presence of backscattering. At higher densities the EMA breaks down as a description of the data. This illustrates that the EMA is essentially a low-density theory, as it was also the case for the percolation models [29–34]. Only for the *stochastic* lattice Lorentz gas does the EMA also yield exact results for the completely filled lattice [9]. Here, the full lattice still has the disorder of different scatterers.

For simulations that run over longer times, the diffusion coefficient $D(t) \equiv \frac{1}{2}\partial_t \langle x^2 \rangle$ decreases! This can not be explained by EMA or other simple kinetic theories. Physically it is clear what is going on: more and more particles find themselves trapped in closed orbits and do not contribute to $D(t)$.

It might be possible that we did not find the right branch of the solution of the coupled equations. However, by varying the starting points we did not find (other) physically relevant solutions. The simulations performed for the set of parameters used for figure 8 show the same effects that we also observed for the other cases

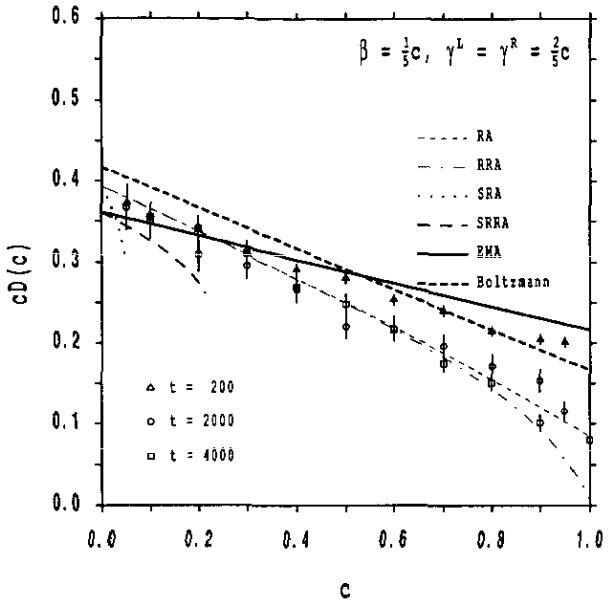

Figure 8. Chiral model with $\beta \neq 0$ and $\gamma^L = \gamma^R$. Simulation results for several values of time t.

discussed before (see figures 3, 5 and 7): the longer we simulate, the lower the diffusion coefficient.

We conclude with some final remarks. First, the chiral model is a model to which the effective medium approximation can be applied in a straightforward manner. The results are expected to be relevant for long times in cases where diffusion, defined in terms of the mean square displacement, exists. This is, however, not the case for all choices for the parameters. Second, the models without backscattering are more likely to show diffusive behaviour than those with backscattering. Third, in the chiral model deviations from the simulation results are observed, contrary to the stochastic model [9]. It is likely that these incorrect predictions by EMA and ring-type kinetic equations are caused by the omission of, for instance, the orbiting collision sequences (see figure 2(*c*)), which account for the periodic orbits in deterministic models, as pointed out in the introduction. Moreover, these trajectories are also fully responsible for the phase space to be split up in separate parts, and thus breaking ergodicity. Fourthly, however, from analyzing the data from computer simulations, one is more and more tempted to question if the model does have diffusive behaviour at all, even in the regions of extended orbits [19, 26].

Acknowledgments

The author acknowledges stimulating discussions with M H Ernst, H van Beijeren and B Nienhuis. The work of the author is financially supported by the Stichting voor Fundamenteel Onderzoek der Materie (FOM), which is sponsored by NWO.

References

[1] Wolfram S 1986 *J. Stat. Phys.* **45** 471; 1984 *Nature* **311** 419

[2] Frisch U, d'Humieres D, Hasslacher N, Lallemand P, Pomeau Y and Rivet J P 1987 *Complex Systems* **1** 649
Henon M 1987 *Complex Systems* **1** 763
Rivet J P 1987 *Complex Systems* **1** 839
[3] Doolen G D, Frisch U, Hasslacher H, Orszag S and Wolfram (eds) 1987 *Lattice Gas Methods for Partial Differential Equations* (New York: Addison-Wesley)
[4] Doolen G D (ed) *Proc. Workshop on Lattice Gas Methods for PDE's, Los Alamos, September 1989* (New York: Addison-Wesley)
[5] Kadanoff L, McNamara G and Zanetti G 1987 *Complex Systems* **1** 791; 1989 *Phys. Rev.* A **40** 4527
[6] Monaco R (ed) 1988 *Proc. Workshop on Discrete Kinetic Theory, Lattice Gas Dynamics and Foundations of Hydrodynamics, Turin* (Singapore: World Scientific)
[7] Ernst M H, van Velzen G A and Binder P M 1989 *Phys. Rev.* A **39** 4327
[8] van Velzen G A and Ernst M H 1988 *Proceedings of the Workshop on Discrete Kinetic Theory, Lattice Gas Dynamics and Foundations of Hydrodynamics* Turin (Singapore: World Scientific)
[9] Ernst M H and van Velzen G A 1989 *J. Phys. A: Math. Gen.* **22** 4611–32
[10] Lorentz H A 1904 *Kon. Acad. Wet. Amsterdam* **13** 493; 1905 *Proc. Amst. Acad.* **7** 438
[11] McLennan J A 1989 *Statistical Mechanics* (New York: Prentice Hall)
[12] Dorfman J R and van Beijeren H 1977 *Statistical Mechanics, Part B: Time dependent processes* ed B J Berne (New York: Plenum) p 65
[13] Sengers J V and Gillespie D T 1977 *Statistical Mechanics, Part B: Time dependent processes* ed B J Berne (New York: Plenum)
[14] van Leeuwen J M J and Weyland A 1967 *Physica* **36A** 457
Weyland A and van Leeuwen J M J 1968 *Physica* **38A** 35
[15] Hauge E H 1974 *Transport Phenomena (Lecture Notes in Physics 31)* ed G Kirczenow and J Marro (Berlin: Springer) p 338
[16] Hauge E H and Cohen E G D 1969 *J. Math. Phys.* **10** 397
[17] Jepsen D W 1965 *J. Math. Phys.* **6** 405
[18] Lebowitz J L and Percus J K 1967 *Phys. Rev.* **155** 122; Lebowitz J L, Percus J K and Sykes J K 1968 *Phys. Rev.* **171** 224
[19] Gunn J M F and Ortuño M 1985 *J. Phys. A: Math. Gen.* **18** L1095
[20] van Velzen G A 1990 *J. Phys. A: Math. Gen.* **23** 4953–76
[21] Nienhuis B private communication
[22] Kong X P and Cohen E G D 1989 *Phys. Rev.* B **40** 4838; *Physica* D submitted
[23] Ruijgrok Th W and Cohen E G D 1988 *Phys. Lett.* **133A** 415
[24] Binder P M 1987 *Complex Systems* **1** 559
[25] Gates D J 1972 *J. Math. Phys.* **13** 1005; 1972 *J. Math. Phys.* **13** 1315
[26] Bouwens B Th, Ernst M H and Binder P N 1989 *Complex Systems* **3**
[27] van Kampen N G 1981 *Stochastic Processes in Physics and Chemistry* (Amsterdam: North-Holland)
[28] Dufty J W and Ernst M H 1989 *J. Phys. Chem.* **93** 7015
[29] Kirkpatrick S 1973 *Rev. Mod. Phys.* **45** 574
[30] Webman I 1981 *Phys. Rev. Lett.* **47** 1496
[31] Haus J W and Kehr K W 1987 *Phys. Rep.* **150** 263
[32] Odagaki T, Lax M and Puri A 1983 *Phys. Rev.* B**28** 2755
[33] Kertész J and Metzger J 1984 *J. Phys. A: Math. Gen.* **17** L501
[34] van Velzen G A, Ernst M H and Dufty J W 1988 *Physica* **154A** 34
[35] Ernst M H, van Velthoven P F J and Nieuwenhuizen Th M 1987 *J. Phys. A: Math. Gen.* **20** 949; 1986 *J. Stat. Phys.* **45** 1001
[36] Ernst M H 1987 *J. Stat. Phys.* **48** 645
[37] van Velzen G A and Ernst M H 1987 *J. Stat. Phys.* **48** 677
[38] Grassberger P 1986 *J. Phys. A: Math. Gen.* **19** 2675
[39] Ziff R M 1986 *Phys. Rev. Lett.* **56** 545
[40] Mood A M, Graybill F A and Boes D C 1974 *Introduction to the Theory of Statistics* (New York: McGraw-Hill) p 76
[41] Ernst M H and van Velzen G A 1989 *J. Stat. Phys.* **57** 455–72